Periodica Polytechnica Chemical Engineering, 69(4), pp. 612–619, 2025

Product Distribution and Quality Changes Induced by UV Pre-Treatment in Waste Tyre Pyrolysis

Csenge Emese Tóth[1]*, Truong Dinh[1], Gábor Nagy[1]

[1] Institute of Energy, Ceramics and Polymer Technology, Faculty of Materials and Chemical Engineering, University of Miskolc, Miskolc-Egyetemváros, H-3515 Miskolc, Hungary
* Corresponding author, e-mail: csenge.emese.toth@uni-miskolc.hu

Received: 31 August 2025, Accepted: 27 November 2025, Published online: 09 December 2025

Abstract

The management of end-of-life tyres represents a growing environmental challenge. Pyrolysis provides a sustainable recycling pathway by converting waste tyres into oil, gas, and char, but the high sulphur content of these products limits their direct utilisation. This study investigates UV irradiation as a pre-treatment method to modify tyre rubber structure and influence subsequent pyrolysis behaviour. Shredded tyre samples were irradiated by UV light for 0, 360, and 1080 min prior to pyrolysis at 900 °C. Structural and morphological changes were characterised using Fourier transform infrared spectroscopy, microscopy, and thermogravimetry. Product yields were quantified, and the resulting oil, char, and gas fractions were analysed by elemental composition, heating value, and gas chromatography. UV pre-treatment induced oxidation, chain scission, and partial devulcanisation in the rubber matrix, leading to more homogeneous thermal degradation. At 900 °C, UV pre-treatment of 1080 min slightly increased gas yields, reduced oil yields, and left char production largely unchanged. Oils from irradiated samples exhibited higher oxygen and sulphur contents, resulting in lower heating values. Char composition remained relatively stable, with heating values of 8–9 MJ/kg. The gas fraction showed increased energy potential but also a higher hydrogen sulphide content. Overall, UV irradiation significantly altered tyre rubber structure and pyrolysis product quality. While the pre-treatment enhanced the energy potential of the gas fraction, it also intensified sulphur-related challenges, underscoring both the potential and limitations of UV-assisted tyre pyrolysis.

Keywords

waste tyre, UV pre-treatment, pyrolysis, FT-IR, TGA

1 Introduction

Global tyre production reached approximately 2.3 billion units in 2022 and is projected to increase to 2.7 billion units by 2028, leading to a continuously growing generation of end-of-life tyres (ELTs) worldwide [1].

Recent assessments report that nearly one billion tyres reach end-of-life each year, while an estimated four billion units remain stockpiled or landfilled worldwide, underscoring the environmental urgency of sustainable recovery routes such as pyrolysis for material and energy valorisation [2, 3]. Vehicle production continues to rise, with over 81 million cars produced in 2022 alone [4], further exacerbating the problem. ELT management poses serious environmental challenges. In the European Union, tyre landfilling has been prohibited since 2006 under Directive 1999/31/EC [5] due to risks of soil and groundwater contamination, fire hazards, and pest proliferation [6]. Extended producer responsibility (EPR) schemes further oblige producers and importers to collect and recycle used tyres [6]. Without proper treatment, tyres degrade very slowly and release harmful compounds such as polycyclic aromatic hydrocarbons (PAHs) into the environment [7–9].

Pyrolysis is one of the most promising recycling routes for waste tyres, converting them into oil, gas, and char [2, 10]. The yields and compositions of these products depend strongly on feedstock properties and operating parameters such as temperature and residence time [6]. These pyrolytic products can partially substitute fossil resources, thereby supporting resource efficiency, the circular economy, and the sustainable development goals [3, 4].

Tyres are complex composites consisting of natural and synthetic rubbers, fillers, vulcanisation agents, and various additives [5, 10]. Approximately half of the tread mass is rubber, primarily natural rubber (NR) and synthetic rubbers such as isoprene rubber (IR), butadiene rubber (BR),

Cite this article as: Tóth, C. E., Dinh, T., Nagy, G. "Product Distribution and Quality Changes Induced by UV Pre-Treatment in Waste Tyre Pyrolysis", Periodica Polytechnica Chemical Engineering, 69(4), pp. 612–619, 2025. https://doi.org/10.3311/PPch.42091

and styrene-butadiene rubber (SBR) [11]. Carbon black is added in large amounts to enhance mechanical strength and wear resistance [12], while sulphur-based vulcanising agents form cross-linked structures that provide thermal stability and tear resistance [12, 13]. Additional additives include fibres, extender oils, and zinc compounds [12].

Sulphur, while essential in tyre manufacturing, presents a major challenge during pyrolysis. It migrates into all product fractions, such as oil, gas, and char, lowering their quality and limiting their direct use [13]. Tyre pyrolysis oil typically contains 1.15–1.24 wt.% sulphur [13], far exceeding fuel standards of 10–15 ppm set in many countries [14]. The sulphur is mainly present as benzothiophene, phenylthiophenes, and dibenzothiophenes, which together account for more than 90% of the sulphur content [15]. In the gas fraction, sulphur is released primarily as hydrogen sulphide (H_2S), carbon disulphide (CS_2), and sulphur dioxide (SO_2), with smaller amounts of carbonyl sulphide (COS) and ethyl mercaptan (C_2H_5SH) [4, 5]. Char mainly contains sulphur in inorganic forms such as zinc sulphide, along with sulphates, aliphatic sulphur, and thiophene sulphur [16].

The chemical complexity of tyres and the broad distribution of sulphur across pyrolytic product streams remain major barriers to efficient valorisation. To address these challenges, various pre-treatment methods have been investigated to enhance product quality and process performance. Among these, ultraviolet (UV) irradiation has garnered particular interest for its ability to modify the surface and chemical structure of polymers [17–20]. In rubbers, UV exposure can induce oxidation, crosslinking, or chain scission [21], promoting the formation of oxygen-containing groups such as alcohols, ketones, and carboxylic acids [22]. NR and butadiene-based polymers are particularly susceptible to UV degradation, generally degrade faster than polychloroprene or styrene-rich materials [17]. UV ageing also reduces extender oils, accelerators, and antioxidants in tyre and road-wear particles, while increasing oxygen and silicon content at the surface [22]. Collectively, these structural and compositional changes can alter thermal decomposition behaviour, thereby influencing pyrolysis kinetics and product yields, and composition.

This study investigates the effect of UV pre-treatment on waste tyre pyrolysis. Shredded tyre samples were subjected to varying UV exposure times and subsequently pyrolysed at 900 °C. Structural and compositional changes were analysed using Fourier-transform infrared (FT-IR) spectroscopy, thermogravimetric analysis (TGA), and CHNS elemental analysis, while product yields and distributions were evaluated with particular focus on carbon redistribution and sulphur content.

2 Materials and methods

2.1 Feedstock and UV pre-treatment

The feedstock was shredded ELT rubber with a particle size of 0.5–2 mm. Elemental analysis of the material showed 78.1 wt.% carbon, 6.9 wt.% hydrogen, 0.5 wt.% nitrogen, 1.2 wt.% sulphur, and 5.4 wt.% oxygen. The measured ash content was 8.6 wt.%, and the higher heating value (HHV) was 38.3 MJ/kg, comparable to conventional fossil fuels. The relatively high sulphur content represents a key challenge for product quality.

UV irradiation was applied as a pre-treatment for 0, 360, and 1080 min prior to pyrolysis. The treatment was conducted in a UV chamber in accordance with the ASTM D4329-13 standard [23]. The UV lamp was positioned at a fixed distance above the material, and the samples were periodically stirred to ensure uniform exposure.

2.2 Pyrolysis procedure

Pyrolysis experiments were carried out in a horizontal tubular reactor constructed from heat-resistant steel (370 mm length, 30 mm inner diameter). The reactor was placed inside an electric resistance tube furnace (Hőker 350/900, Hungary). For each run, 30 ± 1 g of pretreated feedstock was loaded into the reactor. To maintain inert conditions, the system was purged with nitrogen prior to heating. The furnace was then heated at 10 °C/min to 900 °C and held at this temperature for 60 min.

2.3 Analytical techniques

The ash content of the feedstock and products was measured according to EN 14775:2010 [24]. Elemental composition (C, H, N, S, O) of the feedstock, oil, and char was analysed following ISO 16993:2016 [25].

Structural changes in the samples were characterised by FT-IR spectroscopy (Bruker Tensor 27, Germany). Microscopic observations were conducted with a Zeiss Axio Imager (Germany) optical microscope. TGA was performed using a MOM Derivatograph-C (Hungary) instrument.

The composition of the pyrolysis gas (H_2, CO, CO_2, CH_4, C_2–C_6 hydrocarbons) was dissected by fast gas chromatography (Dani Master GC, Germany) equipped with both thermal conductivity detector (TCD) and flame ionisation detector (FID).

3 Results and discussions

3.1 Structural changes after UV pre-treatment

Optical microscopy revealed progressive surface darkening and microcrack formation with increasing irradiation time (Fig. 1). The untreated sample (Fig. 1(a)) exhibited smooth morphology, whereas the surface exposed for 360 min (Fig. 1(b)) showed initial oxidation and localised discolouration. After 1080 min of UV treatment (Fig. 1(c)), a dense crack network and surface roughening became evident, indicating embrittlement and oxidative degradation of the rubber matrix.

The FT-IR spectra of untreated and UV-irradiated tyre samples presented in Fig. 2 showed clear modifications with increasing irradiation time. Several characteristic absorption bands shifted in intensity, indicating oxidation and structural transformation.

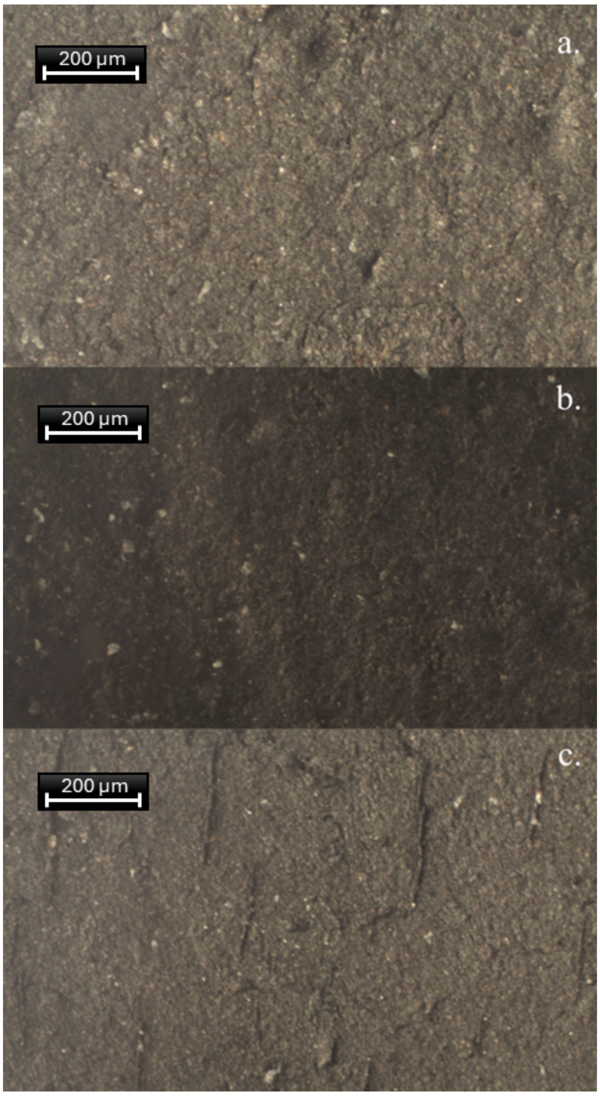

Fig. 1 Microscopic observation of tyre samples after (a) 0 min, (b) 360 min, and (c) 1080 min of UV irradiation

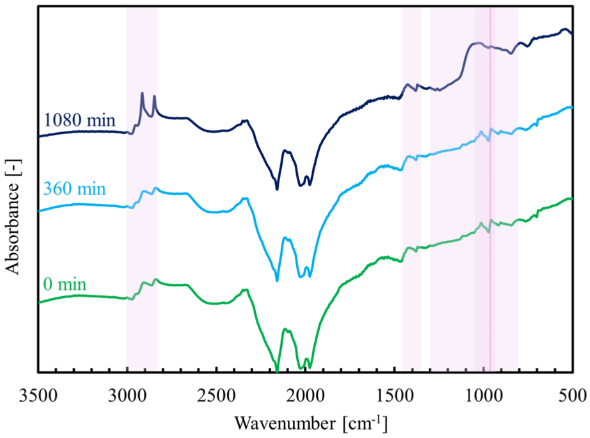

Fig. 2 FTIR spectra of tyre samples after 0, 360, and 1080 min UV pre-treatment

As summarised in Table 1 [8, 17, 26–31], the absorption bands between 808–1060 cm^{-1}, attributed to Si−O−Si vibrations, intensified after irradiation. Similarly, the bands in the 950–1300 cm^{-1} region, associated with C−O stretching and O−H bending, also increased in intensity. In contrast, the band at 967 cm^{-1}, characteristic of 1,4-butadiene units in polybutadiene, decreased, suggesting oxidation and chain scission, which reduce molecular weight and polymer stability.

Additional changes were observed in the 1350–1470 cm^{-1} region, where CH_2 and CH_3 vibrations intensified, also indicating oxidation. A slight decrease in aliphatic C−H stretching bands (2850–3000 cm^{-1}) revealed rearrangements in the hydrocarbon backbone. Moreover, the broad

Table 1 Main FTIR absorption bands of untreated and UV pre-treated tyre samples

Wavenumber [cm^{-1}]	Assignment	Observation after UV treatment	Ref..
808–1060	Symmetric stretching vibration and symmetric stretching vibration Si-O-Si	Increased intensity	[26]
950–1300	C−O stretching and O−H bending	Increased intensity	[27, 28]
967	1,4-butadiene units are being oxidized	Decreased intensity	[17, 29]
1350–1470	CH_2 and CH_3 bonds	Increased intensity	[30]
2850–3000	Aliphatic C−H stretching	Decreased intensity	[8]
3200–3600	O−H stretching	Appearance of new oxygenated groups	[31]

O−H stretching band at 3200–3600 cm^{-1} became more visible, confirming the formation of alcohols, ketones, and carboxylic acids.

Overall, UV pre-treatment initiated oxidative reactions, reduced sulphur bonding, and modified the surface structure of the tyre rubber. These alterations are expected to strongly influence the behaviour of the material during subsequent pyrolysis.

3.2 Thermal behaviour after UV pre-treatment

The thermal degradation of untreated and UV-irradiated tyre samples is represented via the TGA and DTG curves depicted in Fig. 3. The untreated rubber exhibited the highest overall mass loss, while the UV-treated samples displayed greater residual mass at 900 °C, suggesting enhanced thermal stability after irradiation.

The DTG profiles further revealed that the untreated sample decomposed in two distinct stages, whereas UV-treated samples displayed a more uniform, single-step degradation. This shift indicates that photodegradation altered the structure of the rubber, making its decomposition more homogeneous.

These observations are consistent with the FT-IR results, confirming that UV irradiation introduced oxygen-containing groups and weakened sulphur bonds, thereby simplifying the thermal degradation pathway.

The TGA and DTG curves exhibited the typical multi-stage decomposition behaviour of tyre material. The first mass loss below 300 °C corresponded to the evaporation of oils and additives [32].

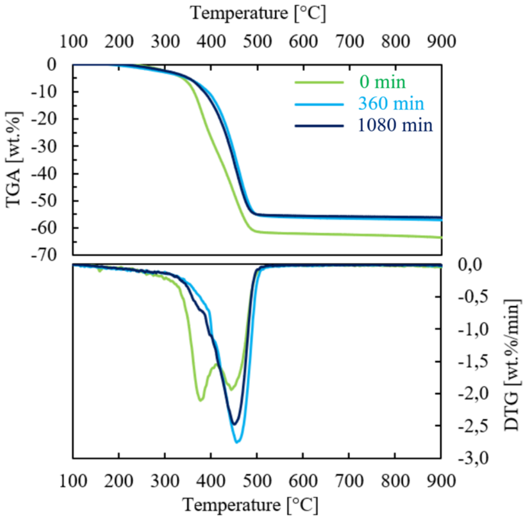

Fig. 3 TGA and DTG curves of tyre rubber samples after 0, 360, and 1080 min of UV pre-treatment

The major degradation, occurring between 350 °C and 520 °C, was associated with the breakdown of rubber polymers. Previous studies identified two overlapping DTG peaks in this range: the first at 380–400 °C, attributed to NR, and the second at 470–490 °C, related to SBR and BR [5, 33]. A third, minor mass-loss above 750 °C was linked to the oxidation of residual carbon black and inorganic fillers, consistent with observations in UV-aged tyre wear particles [22].

Following UV irradiation, the DTG profile showed a reduced intensity, and the two distinct peaks merged into a single, broader maximum. Similar behaviour was reported in earlier studies on UV-aged tyre particles [22], where the NR-related peak (~390 °C) disappeared and the SBR + BR maximum shifted to lower temperatures. This reflects photo-oxidation and partial devulcanisation of the polymer network, which lowers the activation energy required for decomposition. Moreover, oxidation reactions initiated during irradiation promote earlier thermal degradation during heating [32].

3.3 Product distribution

The distribution of pyrolysis products, including char, oil, and gas at 900 °C, is shown in Fig. 4.

Oil was the dominant fraction, followed by char and a smaller proportion of gas. UV irradiation caused only minor changes in yields. After 360 min of treatment, the gas fraction decreased slightly, accompanied by an

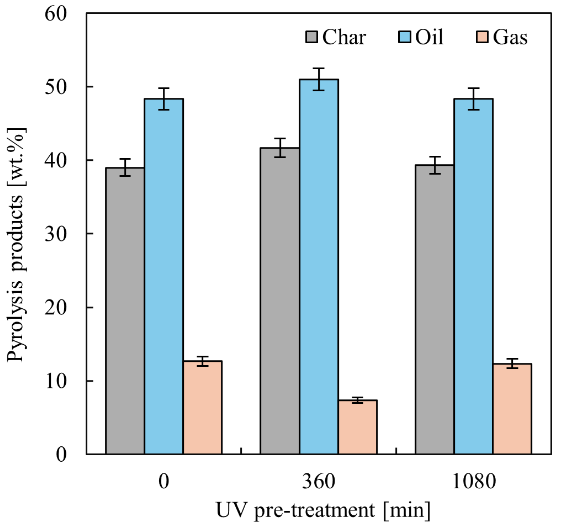

Fig. 4 Distribution of pyrolysis products (char, oil, and gas) at 900 °C after different UV pre-treatment times. Each value represents the average of duplicate experiments (*n* = 3). Standard deviations were below ±1.5 wt.% for all fractions, confirming good reproducibility of the pyrolysis experiments.

increase in oil and char yields. After 1080 min, these trends reversed with the increase of the gas fractions and slight decrease of the oil yield, while the char content remained almost unchanged compared to the sample without irradiation pre-treatment.

These results indicate that at 900 °C, secondary cracking enhances gas formation. UV pre-treatment appears to facilitate this process by promoting volatile release, but the impact of irradiation duration was relatively minor.

3.4 Elemental composition

The elemental composition of pyrolysis oil and char is summarised in Table 2. In the oil fraction, the untreated sample contained 76.5 wt.% carbon and 22.6 wt.% oxygen. After 360 min of UV pre-treatment, the carbon content decreased to 72.9 wt.% while oxygen increased to 25.0 wt.%. At 1080 min, similar values were maintained. Sulphur content also rose from 0.3 wt.% to 1.3–1.4 wt.% after irradiation. These trends indicate that UV pre-treatment promoted oxidation and enriched sulphur concentration in the oil fraction.

On the other hand, the char fraction showed more variable behaviour. The untreated sample contained 67.7 wt.% carbon and 29.3 wt.% oxygen. After 360 min of irradiation, the carbon concentration increased to 72.9 wt.% and oxygen decreased to 25.0 wt.%. While at 1080 min, the composition shifted slightly to 72.5 wt.% carbon and 25.5 wt.% oxygen. Sulphur content declined modestly compared to the untreated char.

Collectively, UV pre-treatment altered the balance between carbon and oxygen in both oil and char fractions. The oil became more oxygen- and sulphur-rich, whereas the char composition exhibited variable trends with exposure time. These compositional changes influence both the energy quality of the products and their potential utilisation as fuels.

Table 2 Elemental composition of pyrolysis oil and char at 900 °C after different UV pre-treatment times. Each value represents the average of duplicate CHNS measurements (*n* = 6).

		UV pre-treatment time [min]					
		0		360		1080	
Oil	C	76.50	±0.52	72.90	±0.50	72.51	±0.52
	H	0.30	±0.02	0.56	±0.03	0.52	±0.03
	N	0.30	±0.01	0.18	±0.02	0.16	±0.02
	S	0.30	±0.01	1.39	±0.04	1.27	±0.03
	O*	22.60	±0.35	24.98	±0.38	25.54	±0.41
Char	C	67.69	±0.47	72.90	±0.50	72.51	±0.52
	H	0.77	±0.04	0.56	±0.03	0.52	±0.03
	N	0.27	±0.02	0.18	±0.02	0.16	±0.02
	S	1.94	±0.05	1.39	±0.04	1.79	±0.03
	O*	29.34	±0.43	24.98	±0.38	25.54	±0.41

*: by difference

3.5 Pyrolysis gas composition

The composition and properties of the pyrolysis gas are presented in Table 3. The major components are hydrogen, methane, light hydrocarbons (C_2–C_4), carbon monoxide, and carbon dioxide, while small amounts of C_5–C_6 hydrocarbons were also detected.

In the untreated sample, hydrogen accounted for 17.6 vol.% of the gas. After 360 min of UV pre-treatment, this value remained nearly unchanged, but subsequently decreased sharply to 4.2 vol.% after 1080 min.

In contrast, methane increased from 15.0 vol.% to 17.4 vol.%, while C_2–C_4 hydrocarbons also became more abundant with increasing irradiation time. Carbon monoxide declined steadily from 6.8 to 2.4 vol.%, whereas carbon dioxide fluctuated between 5.7 and 8.9 vol.%. The H_2/CO ratio first increased from 2.6 to 4.5 and then decreased to 1.8 after the longest exposure.

The heating value of the gas increased from 24.7 to 27.3 MJ m^{-3}, indicating an enhanced energy potential. However, the H_2S concentration rose markedly from 323 ppm to 1600 ppm. Detailed compositional analysis confirmed the enrichment of light hydrocarbons after UV irradiation.

Ethene, propene, and butenes became more prominent than their saturated counterparts, indicating enhanced chain scission and dehydrogenation during pyrolysis. Slight increases in ethane, propane, and butane suggest secondary cracking and partial hydrogenation. Pentanes and hexanes remained below 1 vol.%, indicating limited chain-growth reactions. These observations demonstrate that UV pre-treatment weakens molecular bonds and promotes surface oxidation, facilitating decomposition into smaller fragments during pyrolysis.

The observed reduction in H_2 content and increase in CH_4 fraction are consistent with previous inert TGA studies on UV-aged tyre materials [22]. Overall, UV pre-treatment shifts the gas composition toward lighter, more energetic hydrocarbons, but also increases the sulphur burden in the gas phase.

4 Conclusion

UV irradiation prior to pyrolysis induced significant structural modifications in tyre rubber, as evidenced by

Table 3 Composition and properties of pyrolysis gas after different UV pre-treatment times. Values are reported in vol.% except for H_2S, which is given in ppm. Data are presented as mean ± standard deviation (*n* = 3). "<DL" denotes values below the detection limit (~0.01 vol.%), which were treated as zero for summation. Prefixes "n-", "iso-", and "neo-" refer to isomeric structures. ΣC_2–ΣC_6 indicate the summed fractions of the respective hydrocarbon groups.

Component		UV pre-treatment time [min]					
		0		360		1080	
H_2S	ppm	323	±13	1350	±40	1600	±50
CO	vol.%	6.78	±0.1	4.00	±0.1	2.40	±0.1
CO_2	vol.%	8.86	±0.2	5.69	±0.2	8.35	±0.2
H_2	vol.%	17.62	±0.2	18.04	±0.2	4.20	±0.2
CH_4	vol.%	14.98	±0.3	12.58	±0.3	17.36	±0.3
C_2H_4	vol.%	4.33	±0.2	2.05	±0.2	2.36	±0.2
C_2H_6	vol.%	2.86	±0.2	3.61	±0.2	4.04	±0.2
C_3H_6	vol.%	1.87	±0.1	1.54	±0.1	1.70	±0.1
C_3H_8	vol.%	1.58	±0.1	1.79	±0.1	1.84	±0.1
C_4H_8 (iso)	vol.%	0.44	±0.1	0.44	±0.1	0.45	±0.1
C_4H_8 (1-)	vol.%	5.76	±0.2	8.11	±0.2	8.60	±0.2
C_4H_{10} (iso)	vol.%	0.34	±0.1	0.35	±0.1	0.00	±0.1
C_4H_{10} (n-)	vol.%	0.45	±0.1	0.61	±0.1	0.66	±0.1
C_5H_{10} (1-)	vol.%	<DL	-	0.23	±0.1	0.21	±0.1
C_5H_{10} (trans-2-)	vol.%	0.07	±0.01	0.05	±0.01	0.06	±0.01
C_5H_{12} (neo)	vol.%	<DL	-	0.21	±0.015	0.22	±0.015
C_5H_{12} (iso)	vol.%	<DL	-	0.72	±0.1	0.75	±0.1
C_5H_{12} (n-)	vol.%	<DL	-	0.37	±0.1	0.39	±0.1
C_6H_{12} (1-)	vol.%	<DL	-	0.01	±0.1	0.01	±0.1
C_6H_{14} (n-)	vol.%	0.53	±0.1	0.02	±0.1	0.01	±0.1
ΣC_2	vol.%	7.18	±0.2	5.67	±0.2	6.39	±0.2
ΣC_3	vol.%	3.45	±0.1	3.34	±0.1	3.54	±0.1
ΣC_4	vol.%	6.98	±0.2	9.50	±0.2	9.70	±0.2
ΣC_5	vol.%	0.07	±0.1	1.58	±0.1	1.63	±0.1
ΣC_6	vol.%	0.53	±0.1	0.03	±0.1	0.02	±0.1
H_2/CO ratio	-	2.60	-	4.51	-	1.75	-
HHV	MJ m^{-3}	24.7	-	26.4	-	27.3	-

FT-IR and TGA analyses. The pre-treatment promoted oxidation, chain scission, and a shift toward more homogeneous thermal degradation.

At 900 °C, UV pre-treatment led to slight but clear changes in product distribution. A noticeable increase in the oil and char yields could be seen at 360 min, but at 1080 min, only marginal changes were observed, compared to the sample without pre-treatment.

Elemental analysis indicated that the pre-treatment enriched oxygen and sulphur contents in the oil, whereas the char showed time-dependent variations in composition. The gaseous fraction exhibited higher concentrations of methane and C_2–C_4 hydrocarbons, resulting in greater heating values. However, UV pre-treatment also led to a dramatic increase in H_2S content, which poses challenges for direct utilisation.

In summary, UV pre-treatment significantly influenced both the structure of tyre rubber and the composition and quality of the pyrolysis products. The process enhanced gas calorific value but also increased sulphur transfer, highlighting both advantages and potential drawbacks. Nevertheless, the clear influence of UV energy input on product yield and quality suggests that controlled irradiation may serve as a novel tool for feedstock preparation. Future studies on optimising wavelength, irradiation intensity, and exposure duration, as well as exploring rubber composition effects, can assist in tailoring UV-assisted pre-treatment for specific pyrolysis applications.

Acknowledgement

Supported by the university research scholarship program of the ministry for culture and innovation from the source of the national research, development and innovation fund.

References

[1] Maganinho, C., Silca, C. M. C., Costa, S. M. R., Mendes, A., Rocha, J., Silva, C. M., Portugal, I. "Advances in the pyrolysis of end-of-life tires: A critical review of reactor systems, process conditions and industrial applications", Journal of Environmental Chemical Engineering, 13(5), 118667, 2025. https://doi.org/10.1016/j.jece.2025.118667

[2] Tekin, Z., Gülcan, H. E. "Effect of the use of waste tyre pyrolysis oil and TiO_2-assisted ethylene glycol additive on performance, emissions, energy, exergy, environmental and economic indicators in a gasoline engine", Thermal Science and Engineering Progress, 68, 104197, 2025. https://doi.org/10.1016/j.tsep.2025.104197

[3] Halawy, L., Karroum, W. B., Hijazi, A., Aouad, S., Zeaiter, J. "Catalytic pyrolysis of waste tires over Bi-metallic USY for the production of hydrogen and light gases", Journal of Environmental Chemical Engineering, 13(6), 119418, 2025. https://doi.org/10.1016/j.jece.2025.119418

[4] Hu, Y., Yu, X., Ren, J., Zeng, Z., Qian, Q. "Waste tire valorization: Advanced technologies, process simulation, system optimization, and sustainability", Science of The Total Environment, 942, 173561, 2024. https://doi.org/10.1016/j.scitotenv.2024.173561

[5] Sanchís, A., Navarro, M. V., Veses, A., Martínez, J. D., Callén, M. S., López, J. M., García, T., Murillo, R. "Pyrolysis of different types and sections of end-of-life tyres: Kinetics and experiments to improve product quality", Journal of Analytical and Applied Pyrolysis, 192, 107309, 2025. https://doi.org/10.1016/j.jaap.2025.107309

[6] Bockstal, L., Berchem, T., Schmetz, Q., Richel, A. "Devulcanisation and reclaiming of tires and rubber by physical and chemical processes: A review", Journal of Cleaner Production, 236, 117574, 2019. https://doi.org/10.1016/j.jclepro.2019.07.049

[7] Farooq, M. Z., Yu, H., Lin, F., Rajput, M. I., Kumar, A., Chen, G. "Kinetic insights and pollution mitigation in waste tire pyrolysis: Targeting sulfur, nitrogen, and PAHs emissions", Journal of Analytical and Applied Pyrolysis, 181, 106626, 2024. https://doi.org/10.1016/j.jaap.2024.106626

[8] Zhang, Q., Xu, X., Song, C., Zhang, D., Kong, Y., Cui, X. "Effect of UV exposure and natural aging on the in vitro PAHs bioaccessibility associated with tire wear particles in soil", Science of The Total Environment, 951, 175751, 2024. https://doi.org/10.1016/j.scitotenv.2024.175751

[9] Nadal, M., Rovira, J., Díaz-Ferrero, J., Schuhmacher, M., Domingo, J. L. "Human exposure to environmental pollutants after a tire landfill fire in Spain: Health risks", Environment International, 97, pp. 37–44, 2016. https://doi.org/10.1016/j.envint.2016.10.016

[10] Zerin, N. H., Rasul, M. G., Jahirul, M. I., Sayem, A. S. M. "End-of-life tyre conversion to energy: A review on pyrolysis and activated carbon production processes and their challenges", Science of The Total Environment, 905, 166981, 2023. https://doi.org/10.1016/j.scitotenv.2023.166981

[11] Thornton, S. A., Milton, S. G., Lautermilch, L. R., Massarsky, A., Unice, K. M. "Pyrolysis-GC/MS calibration for environmental quantification of tire tread: Standards and marketplace averaged elastomer subunit profiles", Chemosphere, 385, 144554, 2025. https://doi.org/10.1016/j.chemosphere.2025.144554

[12] Fu, J., Je, W., Ji, L., Yin, Y., Xu, X., Huang, Q., Li, X., Jiao, W., Zhan, M. "Characteristics of the pyrolytic products and the pollutant emissions at different operating stages from a pilot waste tire pyrolysis furnace", Waste Management, 174, pp. 585–596, 2024. https://doi.org/10.1016/j.wasman.2023.12.023

[13] Dewi, W. N., Zhou, Q., Mollah, M., Yang, S., Ilankoon, I. M. S. K., Chaffee, A., Zhang, L. "Synergistic interaction between scrap tyre and plastics for the production of sulphur-free, light oil from fast co-pyrolysis", Waste Management, 179, pp. 99–109, 2024. https://doi.org/10.1016/j.wasman.2024.03.007

[14] Sinurat, S., Hafriz, R. S. R. M., Habib, S. H., Salmiaton, A., Izhar, S., Hamid, M. R. A., Sobri, S., Razali, N. M. "Preparation of a single metal catalyst loaded on alumina support to refine waste tire pyrolysis oil (WTPO) via catalytic hydrogenation", Journal of Analytical and Applied Pyrolysis, 176, 106236, 2023. https://doi.org/10.1016/j.jaap.2023.106236

[15] Jiang, H., Zhang, J., Shao, J., Fan, T., Li, J., Agblevor, F., Song, H., Yu, J., Yang, H., Chen, H. "Desulfurization and upgrade of pyrolytic oil and gas during waste tires pyrolysis: The role of metal oxides", Waste Management, 182, pp. 44–54, 2024. https://doi.org/10.1016/j.wasman.2024.04.020

[16] Li, Y., Nahil, M. A., Williams, P. T. "Pyrolysis-catalytic steam reforming of waste plastics for enhanced hydrogen/syngas yield using sacrificial tire pyrolysis char catalyst", Chemical Engineering Journal, 467, 143427, 2023. https://doi.org/10.1016/j.cej.2023.143427

[17] Wypych, G. (ed.) "Handbook of UV Degradation and Stabilization", ChemTec Publishing, 2020. https://doi.org/10.1016/B978-1-927885-57-4.50004-8

[18] Rabek, J. F. "Photodegradation of Polymers", Berlin, Heidelberg: Springer, 1996. https://doi.org/10.1007/978-3-642-80090-0

[19] dos Santos, K. A. M., Suarez, P. A. Z., J. Rubim, C. "Photodegradation of synthetic and natural polyisoprenes at specific UV radiations", Polymer Degradation and Stability, 90(1), pp. 34–43, 2005. https://doi.org/10.1016/j.polymdegradstab.2005.01.038

[20] Kuyyakanont, A., Iwata, M. "Study of different degradation effects in UV-sensitive polymers using xenon lamp and deuterium lamp to simulate UV irradiation in space environment", Nuclear Instruments and Methods in Physics Research Section B: Beam Interactions with Materials and Atoms, 549, 165267, 2024. https://doi.org/10.1016/j.nimb.2024.165267

[21] Ossola, G., Wojcik, A. "UV modification of tire rubber for use in cementitious composites", Cement and Concrete Composites, 52, pp. 34–41, 2014. https://doi.org/10.1016/j.cemconcomp.2014.04.004

[22] van Os, M. F., Nooijens, M. G. E., van Duivenbode, A. v. R., Tromp, P. C., Höppener, E. M., Grigoriadi, K., Boersma, A., Parker, L. A. "Degradation rates and ageing effects of UV on tyre and road wear particles", Chemosphere, 372, 144121, 2025. https://doi.org/10.1016/j.chemosphere.2025.144121

[23] ASTM "ASTM D4329-13 Standard Practice for Fluorescent Ultraviolet (UV) Lamp Apparatus Exposure of Plastics", ASTM International, West Conshohocken, PA, USA, 2013. https://doi.org/10.1520/D4329-13

[24] CEN "EN 14775:2010 Solid biofuels - Method for the determination of ash content", European Committee for Standardization, Brussels, Belgium, 2010.

[25] ISO "ISO 16993:2016 Solid biofuels — Conversion of analytical results from one basis to another", International Organization for Standardization, Geneva, Switzerland, 2016.

[26] Tamizhdurai, P., Arthi, P., Mangesh, V. L., Krishnan, P. S., …, Kumaran, R. "Clean energy technology: Hydro-processing of waste tyre pyrolysis oil (WTPO) to diesel fuel in a continuous reactor using Co/SBA-15 catalyst", Applications in Energy and Combustion Science, 21, 100305, 2025. https://doi.org/10.1016/j.jaecs.2024.100305

[27] Alzahrani, N., Nahil, M. A., Williams, P. T. "Co-pyrolysis of waste plastics and tires: Influence of interaction on product oil and gas composition", Journal of the Energy Institute, 118, 101908, 2025. https://doi.org/10.1016/j.joei.2024.101908

[28] Fan, X., Ma, Z., Zou, Y., Liu, J., Hou, J. "Investigation on the adsorption and desorption behaviors of heavy metals by tire wear particles with or without UV ageing processes", Environmental Research, 195, 110858, 2021. https://doi.org/10.1016/j.envres.2021.110858

[29] Neral, B., Šostar-Turk, S., Vončina, B. "Properties of UV-cured pigment prints on textile fabric", Dyes and Pigments, 68(2–3), pp. 143–150, 2006. https://doi.org/10.1016/j.dyepig.2005.01.022

[30] Mohan, A., Dutta, S., Madav, V., Bhushnoo, S., Fernandez-Garcia, J., Williams, P. "Co-pyrolysis of scrap tire and plastic using coal derived flyash", In: EUBCE 2019 Online Conference Proceedings. 27th European Biomass Conference & Exhibition, 2019, pp. 1501–1506.

[31] Kuptsov, A. H., Zhizhin, G. N. "Handbook of Fourier Transform Raman and Infrared Spectra of Polymers", Elsevier, 1998. [online] Available at: https://shop.elsevier.com/books/handbook-of-fourier-transform-raman-and-infrared-spectra-of-polymers/kuptsov/978-0-444-82620-6 [Accessed: 27 October 2024]

[32] Thomas, J., Moosavian, S. K., Cutright, T., Pugh, C., Soucek, M. D. "Investigation of abiotic degradation of tire cryogrinds", Polymer Degradation and Stability, 195, 109814, 2022. https://doi.org/10.1016/j.polymdegradstab.2021.109814

[33] Sun, D., Kandare, E., Maniam, S., Zhou, A., Robert, D., Buddhacosa, N., Giustozzi, F. "Thermal-based experimental method and kinetic model for predicting the composition of crumb rubber derived from end-of-life vehicle tyres", Journal of Cleaner Production, 357, 132002, 2022. https://doi.org/10.1016/j.jclepro.2022.132002